Article:
Ma, Y, Chen, XH orcid.org/0000-0002-2053-2448 and Yu, HS orcid.org/0000-0003-3330-1531 (2020) An extension of Biot's theory with molecular influence based on mixture coupling theory: Mathematical model. International Journal of Solids and Structures, 191-192. pp. 76-86. ISSN 0020-7683

https://doi.org/10.1016/j.ijsolstr.2019.11.015

An extension of Biot's Theory with molecular influence based on Mixture Coupling Theory: Mathematical model

Yue Ma, Xiao-Hui Chen*, Hai-Sui Yu

*School of Civil Engineering, University of Leeds, UK

*Telephone: +44 (0)113 3430350

*Email: x.chen@leeds.ac.uk

Abstract

Biot's hydro-mechanical coupled consolidation theory has been widely used in Geotechnical Engineering for nearly 100 years. However, the Chemically Disturbed Zone (CDZ) generated in many geotechnical engineering applications (e.g. nuclear waste disposal, carbon capture and storage etc.) are not considered by Biot's theory, especially where there are highly swelling rocks (e.g. shale) and dissolving minerals. This paper presents a rigorous fundamental extension of Biots consolidation theory, with comprehensively considering the influence of molecular processes of coupled swelling and mineral dissolution, based on the newly developed Mixture Coupling Theory. A simple numerical example has been used for the demonstration purpose of the new constitutive equations, and the result shows that molecular influence can have a significant impact on the mechanical performance of the rocks.

Keywords: Unsaturated, Biot's theory; Mixture Coupling Theory; Swelling; Dissolution

1 Introduction

Many contemporary geotechnical engineering applications create a Chemical Disturbed Zone (CDZ), where chemical reactions occurring at the molecular scale strongly change the engineering properties of rocks/soils (NNL, 2016). Applications include carbon capture and storage, shale gas extraction, acid mine drainage, nuclear waste disposal, hyper alkaline industrial wastes (e.g. steel slags and “red muds” from aluminum extraction), and accidental chemical spills (Chen et al., 2015; Moyce et al., 2014).

Minerals in rocks/soils may dissolve into groundwater until they reach thermodynamic equilibrium (Yadav and Chakrapani, 2006). Most minerals react slowly in groundwater, however, when the pore fluid is replaced by reactive solutions or the life cycle of the engineering application is long enough (e.g. 100 years for nuclear waste disposal), the chemical processes will result in significant changes to the physical properties of the ground (e.g. the porosity, permeability, and strength) (Emmanuel and Berkowitz, 2007; Fredd and Fogler, 1998; Zhao, 2014).

Swelling of rocks/soils is another engineering problem caused by molecular influence. Typically, two major mechanisms of swelling are observed in the clay platelets within a soil/rock, i.e. hydration swelling and osmotic swelling (Chen, 2013). Hydration swelling is the result of exchangeable cations of the dry clay. One to four water layers can be added between clay platelets due to cations hydrate, resulting in the space between clay layers. Osmotic swelling is resulted from the large difference of the ion concentration close to the clay surfaces or in the pore water. Fig. 1 briefly illustrates hydration swelling and osmotic swelling.

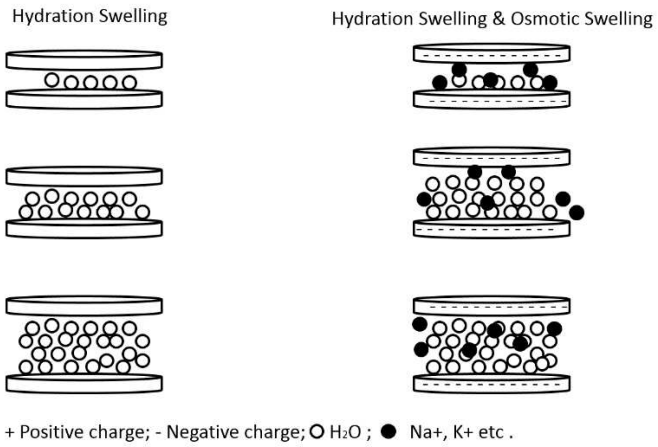

Fig 1. hydration swelling and osmotic swelling

Swelling is coupled with the dissolving process. Dissolved minerals release large amounts of cations or anions into pore water or clay platelets, and these chemicals will change the flow direction of H_2O due to osmotic flow, resulting in osmotic swelling. Meanwhile, the new absorbed water diluting the solute which was in equilibrium with the minerals, allows more minerals to be dissolved towards a new equilibrium. Such interactions between swelling and dissolution remain a challenge due to multiscale physical-chemical coupling.

Traditionally, two major approaches have been developed to describe hydro-mechanical coupling in porous media: the mechanics approach, which is based on the classical consolidation theory of Terzaghi and Biot (Biot, 1962; Biot and Temple, 1972; Terzaghi, 1943), and Mixture theory, which was developed by Truesdell, extended and modified by Humphrey and Rajagopal (Humphrey and Rajagopal, 2002, 2003; Rajagopal, 2007). Lots of researches in Geotechnical Engineering have been focussed on hydro-mechanical coupling using mechanical approach (Graziani and Boldini, 2011; Lewis and Schrefler, 1987b; Meroi et al., 1995; Sanavia et al., 2002), as well as more complicated models considering thermal or chemical couplings (Huyghe and Janssen, 1999; Seetharam et al., 2007). However, the mechanical approach is

not based on a unified systemic theory and does not have the capacity of couplings crossing multiple-disciplines and multiple-scales (Laloui et al., 2003). The interactive element between hydro-mechanical is macroscale level pressure, whereas the interactive element between chemical or/and thermal is the microscale molecular force. The mechanical approach has difficulties of building links between the two scale-levels interactive element, therefore, it has to borrow formulations from other research field when dealing with chemical or/and thermal coupling, due to the gap between Geomechanics and Geochemistry. As a result, the formulations developed are not rigorously mathematically derived, but highly semi-empirical and heavily relying on experiments.

Mixture theory maintains the individuality of the solid and fluid phase and takes account of phase interaction effect (Grasley et al., 2011; Grasley and Rajagopal, 2012; Rajagopal and Tao, 2005; Rajagopal and Tao, 1995). It adopts an 'energy approach' to build a link between microscale molecular force and macro-level pressure. However, this "energy" approach has the difficulty of obtaining detailed information on the interaction between phases, which restrains its applications.

To overcome the challenge, Heidug and Wong(Heidug and Wong, 1996) view a fluid-infiltrated rock as a single continuum and does not explicitly discriminate between the solid and fluid phases. This approach is referred to as modified mixture theory. This theory has been lately extended and reformed with attention on physical-chemical coupling and entropy evolution, and renamed as Mixture Coupling Theory by Chen et al. (Chen, 2010, 2013; Chen and Hicks, 2010; Chen et al., 2018a; Chen et al., 2018b).

Another challenge is the gap between microscale and macroscale(Lewis and Schrefler, 1987b): The hydro-mechanical coupling is at macroscale level, whereas the interaction

between chemicals or/and thermal fields is on the microscale. Thermodynamically Constrained Averaging Theory (TCAT) of Gray and Miller (Gray and Miller, 2014; Gray et al., 2013; Miller et al., 2018) provides a rigorous way of bridging the gap. Mixture coupling theory develops another scope of the average method using non-equilibrium thermodynamics (Chen et al., 2016). It uses entropy production for the dissipation process and Helmholtz free energy to engage mechanical energy which enables well-accepted continuum mechanics to be used for mechanical deformation (e.g. large deformation), leading to a simpler derivation process compared with TCAT. Mixture Coupling Theory has an advantage in physical-chemical coupling process, through using Gibbs-Duhem equation to link chemical potential (rather than molecular forces) with physical thermodynamic properties.

In this paper, a novel mathematical formulation of hydro-mechanical coupled model base on Mixture Coupling Theory is obtained, and the strong couplings between mineral dissolution and swelling are included. Helmholtz free energy is used to give the relationship between these couplings. The fully coupled formulations, which include dissolving and swelling, are obtained. Finally, finite elements are used to solve the governing equations for the demonstration purpose. The results show that both swelling and dissolving have a significant influence on the stress and strain change of the porous media rock.

2 Balance equations and dissipative process

A microscopic domain *V,* which is assumed to be big enough to include solid, water and gas, has been selected within the rock, with the assumption that *S* is its boundary attached to the solid phase, allowing the only movement of fluid (e.g. water, chemicals) across. To simplify the discussion, the air phase is assumed to be continuous with atmospheric pressure $\mathrm{p}_{\mathrm{atm}} = 0$ (Neuman, 1975; Safai and Pinder, 1979)

2.1 Balance equations for energy and mass

Helmholtz free energy combines internal energy and entropy (Haase, 1990). The balance equation can be derived based on the assumption of ignoring gas transport as:

(1) The balance equation can be derived based on the assumption of ignoring gas transport as (Chen, 2013; Chen and Hicks, 2009):

$$\frac{\mathrm{D}}{\mathrm{Dt}}\int_{\mathrm{V}}\psi \mathrm{dV} = \int_{\mathrm{S}}\boldsymbol{\sigma}\mathbf{n}\cdot\mathbf{v}^{\mathrm{s}}\mathrm{dS} - \int_{\mathrm{S}}\mu\mathbf{I}^{\mathrm{w}}\cdot\mathbf{n}\mathrm{dS} - \int_{\mathrm{S}}\mu^{\mathrm{s}}\mathbf{I}^{\mathrm{d}}\cdot\mathbf{n}\mathrm{dS} - \mathrm{T}\int_{\mathrm{V}}\gamma\mathrm{dV} \tag{1}$$

where ψ is Helmholtz free energy density, $\boldsymbol{\sigma}$ is the Cauchy stress tensor, $\mathbf{v}^{\mathrm{s}}$ is the velocity of the solid, $\mathbf{v}^{\mathrm{w}}$ is the velocity of the water, $\mathbf{v}^{\mathrm{s}}$ is the velocity of the solid, μ is the chemical potential of water, μ^{s} is the chemical potential of dissolved solid, T is temperature, γ is the entropy production per unit volume, and the time derivative is

$$\frac{\mathrm{D}}{\mathrm{Dt}} = \partial_{\mathrm{t}} + \mathbf{v}^{\mathrm{s}}\cdot\nabla \tag{2}$$

in which ∂_{t} is the time derivative and ∇ the gradient.

In equation (1), $\mathbf{I}^{\mathrm{w}}$ and $\mathbf{I}^{\mathrm{d}}$ are the mass flux of water and dissolved solid that can be defined as

$$\mathbf{I}^{w} = \rho^{w}(\mathbf{v}^{w} - \mathbf{v}^{s}), \text{ and } \mathbf{I}^{d} = \rho^{d}(\mathbf{v}^{d} - \mathbf{v}^{s}) \tag{3}$$

where ρ^{w} and ρ^{d} are the mass density of water and the dissolved chemical.

The derivative version of the balance equation (1) for the free energy is expressed as

$$\dot{\psi} + \psi\nabla\cdot\mathbf{v}^{s} - \nabla\cdot(\boldsymbol{\sigma}\mathbf{v}^{s}) + \nabla\cdot(\mu\mathbf{I}^{w}) + \nabla\cdot(\mu^{s}\mathbf{I}^{d}) = -T\gamma \le 0 \tag{4}$$

(2) Balance equation for solid mass is

$$\frac{D}{Dt}\left(\int_{V}\rho^{s}dV\right) = -\int_{S}\mathbf{I}^{d}\cdot\mathbf{n}da \tag{5}$$

and the derivative version is

$$\dot{\rho}^{s} + \rho^{s}\tilde{\nabla}\times\mathbf{v}^{s} + \tilde{\nabla}\times\mathbf{I}^{d} = 0 \tag{6}$$

where ρ^{s} is the solid density relative to the unit volume of the fluid-solid-gas mixture.

(3) Balance equation for water mass is

$$\frac{D}{Dt}\left(\int_{V}\rho^{w}dV\right) = -\int_{S}\mathbf{I}^{w}\cdot\mathbf{n}da \tag{7}$$

The derivative version is

$$\dot{\rho}^{w} + \rho^{w}\tilde{\nabla}\times\mathbf{v}^{s} + \tilde{\nabla}\times\mathbf{I}^{w} = 0 \tag{8}$$

The mass density of water ρ^{w} is defined relative to the unit volume of the mixture. It is related to the true mass density ρ_{t}^{w} (relative to the water volume of the mixture) through

$$\rho^{w} = \phi^{w}\rho_{t}^{w} \tag{9}$$

in which ϕ^{w} is the volume fraction of water. The relationship between ϕ^{w} and the porosity of the medium ϕ is

$$\phi^{w} = S^{w}\phi \tag{10}$$

where S^{w} is the saturation of water.

2.2 Dissipative process

This dissipation mechanism at the solid/fluid boundary (e.g. solid/fluid and water/dissolve solid) can be obtained by using non-equilibrium thermodynamics, and the entropy production is described as (Katachalsky and Curran, 1965)

$$0 \le \mathrm{T}\gamma = -\mathbf{I}^{\mathrm{w}} \cdot \nabla\mu - \mathbf{I}^{\mathrm{d}} \cdot \nabla\mu^{\mathrm{s}} \tag{11}$$

where μ^{w} and μ^{d} are the chemical potential of the water and dissolved solids, respectively.

If the chemical transport of dissolved solids is ignored, the equation (11) becomes

$$`0 \le \mathrm{T}\gamma = -\mathbf{I}^{\mathrm{w}} \cdot \nabla\mu \tag{12}$$

Through using Phenomenological relationship for equation (12), and Gibbs-Duhem equation for the pore water giving the relationship between water pressure and water chemical potential, Darcy's law can be obtained as (Chen, 2013)

$$\mathbf{u}_{\mathrm{D}} = -\frac{\mathbf{K}\mathrm{k}_{\mathrm{rw}}}{\mu}\nabla \mathrm{p}_{\mathrm{p}} \tag{13}$$

where $\mathbf{u}_{\mathrm{D}}$ is Darcy's velocity, $\mathbf{K}$ is the permeability, k_{rw} is the relative permeability, and p_{p} is the pore pressure. Note here: The chemical transport is not considered here to simplify the discussion.

3 State equations for swelling and dissolving

There are two types of water in a swelling/dissolving rock; 1) water in the pores which can be described using non-equilibrium thermodynamics, and 2) water in the clay platelets which has a strong feel of intermolecular and surface forces and thermodynamics is not applied (Israelachvili, 1991) (Figure 2). The solids can be classed as two types; 1) the solid skeleton which follows the continuum thermodynamics (mechanics) and 2) the dissolved solid into water that follows the intermolecular or surface forces. (Figure 2).

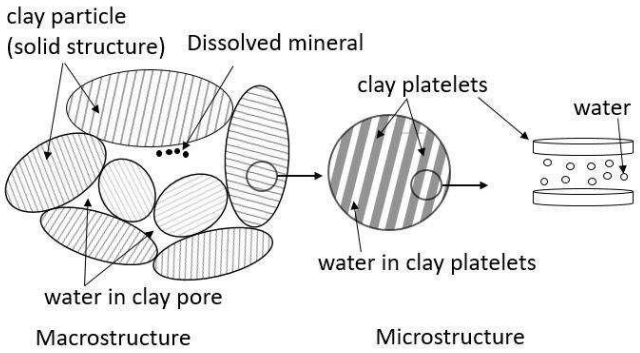

Fig 2. Water types and solid types

3.1 Helmholtz free energy of pore fluid

Based on classical thermodynamics, the Helmholtz free energy density in the pore space (ψ_{pore}) can be written as

$$\psi_{\text{pore}} = -\bar{\text{p}} + \text{S}^{\text{w}}\rho_{\text{t}}^{\text{pore}}(\mu + \mu^{\text{s}}) \tag{14}$$

where the $\rho_{\text{t}}^{\text{pore}}$ (including water and the dissolved solid) is the fluid mass density per unit fluid volume, $\bar{\text{p}}$ is the average pressure in pore space and the gas pressure has been ignored.

The time derivative of equation (14) is

$$\dot{\psi}_{\text{pore}} = -\dot{\bar{p}} + \dot{\mu} S^w \rho_t^{\text{pore}} + \mu (S^w \rho_t^{\text{pore}})^{\cdot} + \dot{\mu}^s S^w \rho_t^{\text{pore}} + \mu^s (S^w \rho_t^{\text{pore}})^{\cdot} \tag{15}$$

Using the Gibbs-Duhem equation for the pore water, this leads to

$$\dot{\bar{p}} = S^w r_t^{\text{pore}} \dot{m} + S^w r_t^{\text{pore}} \dot{\alpha} \tag{16}$$

and the relationship between chemical potential and average pressure as

$$\dot{\mu} + \dot{\mu}^s = \left(\frac{1}{S^w \rho_t^{\text{pore}}}\right) \dot{\bar{p}} \tag{17}$$

Substituting equation (16) into (15), the time derivative of Helmholtz free energy can be simplified as

$$\dot{\psi}_{\text{pore}} = \mu (S^w \rho_t^{\text{pore}})^{\cdot} + \mu^s (S^w \rho_t^{\text{pore}})^{\cdot} \tag{18}$$

3.2 Helmholtz free energy of the whole mixture

It is assumed that the rock maintains mechanical equilibrium so that $\nabla \cdot \boldsymbol{\sigma} = \mathbf{0}$. By substituting the entropy production equation (11) into the Helmholtz free energy balance equation (4) for the mixture, and ignoring $\mathbf{I}^d$ for chemical transport, this leads to

$$\dot{\psi} + \psi \nabla \cdot \mathbf{v}^s - \left(\boldsymbol{\sigma} : \nabla \mathbf{v}^s\right) + \mu \nabla \cdot \mathbf{I}^w = 0 \tag{19}$$

Equation (19) is the free energy at current configuration. To measured the rock's deformation state, classic continuum mechanics has been considered here: an arbitrary reference configuration $\mathbf{X}$ is selected, then at the time t the position is $\mathbf{x}$. The expression of Green strain $\mathbf{E}$, the deformation gradient $\mathbf{F}$,

$$\mathbf{F} = \frac{\partial \mathbf{x}}{\partial \mathbf{X}}(\mathbf{X}, t), \ \mathbf{E} = \frac{1}{2}(\mathbf{F}^{\mathbf{T}}\mathbf{F} - \mathbf{I}), \tag{20}$$

where I is a unit tensor. The relationship between second Piola-Kirchhoff stress $\mathbf{T}$ and Cauchy stress $\boldsymbol{\sigma}$ is

$$\mathbf{T} = \mathrm{J}\mathbf{F}^{-1}\boldsymbol{\sigma}\mathbf{F}^{-\mathrm{T}}$$

where J (the Jacobian of $\mathbf{F}$) is

$$J = \frac{dV}{dV_0}, \quad \dot{J} = J \operatorname{div} v_s$$

By further considering partial masses equation(8) and equation(19), along with the equation (20), it leads to

$$\dot{\Psi} = \operatorname{tr}(\mathbf{T}\dot{\mathbf{E}}) + m\dot{\mu} \tag{21}$$

$$\Psi = J\psi, \quad m = J\rho = JS^w\phi\rho_t^w \tag{22}$$

3.3 Free energy density of the wetted mineral matrix

The free energy of the mineral matrix includes the fluid 'bounded' between clay platelet and the solids dissolved into the platelet. It can be obtained by subtracting the free energy of pore water (section 3.1) from the total free energy of the rock/ fluid (section 3.2).

Therefore, the free energy density of the wetted mineral matrix is written as

$$(\dot{\Psi} - J f^w \dot{\psi}_{pore}) = \operatorname{tr}(\mathbf{T}\dot{\mathbf{E}}) + m\dot{\mu}_{bound} + \bar{p}\dot{\upsilon} + m^s\dot{\mu}_{dissolve} \tag{23}$$

where $\upsilon = J\phi$ is denoted as pore volume per unit referential volume.

For the reason of convenience, the dual potential (deformation energy) can be expressed as

$$W = (\Psi - J\phi^w\psi_f) - \bar{p}\upsilon - \mu\, m_{bound} + \mu^s m_{dissolve} \tag{24}$$

where W is a function of $\mathbf{E}$, $\bar{p}$, μ, μ^s so the expression of $\mathbf{T}$, υ, m_{bound}, $m_{dissolve}$ can be given**.** Equation (24) implies the time derivative of $W(\mathbf{E}, \bar{p}, \mu)$ satisfies the relation

$$\dot{W}(\mathbf{E}, \bar{p}, m, m^s) = \operatorname{tr}(\mathbf{T}\dot{\mathbf{E}}) - \dot{\bar{p}}\upsilon - \bar{p}\dot{\upsilon} - \dot{\mu}m_{bound} + \mu\dot{m}_{dissolve} \tag{25}$$

Hense,

$$T_{ij} = \left(\frac{\partial W}{\partial E_{ij}}\right)_{\bar{p},\mu,\mu^s}, \upsilon = -\left(\frac{\partial W}{\partial \bar{p}}\right)_{E_{ij},\mu,\mu^s}, m_{bound} = -\left(\frac{\partial W}{\partial \mu}\right)_{E_{ij},\bar{p},\mu^s}, m_{dissolve} = \left(\frac{\partial W}{\partial \mu^s}\right)_{E_{ij},\bar{p},\mu} \tag{26}$$

and

$$\dot{W}(\mathbf{E}, \bar{p}, m, m^s) = \left(\frac{\partial W}{\partial E_{ij}}\right)_{\bar{p},m,m^s} \dot{E}_{ij} + \left(\frac{\partial W}{\partial \bar{p}}\right)_{E_{ij},m,m^s} \dot{\bar{p}} + \left(\frac{\partial W}{\partial m}\right)_{E_{ij},\bar{p},m^s} \dot{m} + \left(\frac{\partial W}{\partial m^s}\right)_{E_{ij},\bar{p},m} \dot{m}^s \tag{27}$$

If equation (26) is differentiated respect to time, and by substituting equation (27) into (26), the fundamental constitutive equations for the evolution of stress, pore volume fraction, mass densities of the bounded water and the mass density of dissolved solids can be obtained as (see derivation details in the appendix)

$$\dot{T}_{ij} = L_{ijkl}\dot{E}_{kl} - M_{ij}\dot{\bar{p}} + S_{ij}\dot{m} + H_{ij}\dot{m}^s \tag{28}$$

$$\dot{\upsilon} = M_{ij}\dot{E}_{ij} + Q\dot{\bar{p}} + B\dot{m} + B^s\dot{m}^s \tag{29}$$

$$\dot{m}_{bound} = -S_{ij}\dot{E}_{ij} + B\dot{\bar{p}} + Z\dot{m} + X\dot{m}^s \tag{30}$$

$$\dot{m}_{dissolve} = H_{ij}\dot{E}_{ij} - B^s\dot{\bar{p}} + X\dot{m} + Y\dot{m}^s \tag{31}$$

where the parameters L_{ijkl}, M_{ij}, S_{ij}, H_{ij}, B, X, Y, Z, are defined as following equations

$$L_{ijkl} = \left(\frac{\partial T_{ij}}{\partial E_{kl}}\right)_{\bar{p},\mu,\mu^s} = \left(\frac{\partial T_{kl}}{\partial E_{ij}}\right)_{\bar{p},\mu,\mu^s}$$

$$M_{ij} = -\left(\frac{\partial T_{ij}}{\partial \bar{p}}\right)_{E_{ij},\mu,\mu^s} = \left(\frac{\partial \upsilon}{\partial E_{ij}}\right)_{\bar{p},\mu,\mu^s}$$

$$S_{ij} = \left(\frac{\partial T_{ij}}{\partial \mu}\right)_{E_{ij},\bar{p},\mu^s} = -\left(\frac{\partial m_{bound}}{\partial E_{ij}}\right)_{\bar{p},\mu,\mu^s}$$

$$H_{ij} = \left(\frac{\partial T_{ij}}{\partial \mu^s}\right)_{E_{ij},\bar{p},\mu} = \left(\frac{\partial m_{dissolve}}{\partial E_{ij}}\right)_{\bar{p},\mu,\mu^s} \tag{32}$$

$$Z = \left(\frac{\partial m_{bound}}{\partial \mu} \right)_{E_{ij}, \bar{p}, \mu^s}$$

$$B = \left(\frac{\partial \upsilon}{\partial \mu} \right)_{E_{ij}, \bar{p}, \mu^s} = \left(\frac{\partial m_{bound}}{\partial \bar{p}} \right)_{E_{ij}, \mu, \mu^s}$$

$$Q = \left(\frac{\partial \upsilon}{\partial \bar{p}} \right)_{E_{ij}, \mu}$$

$$Y = \left(\frac{\partial m_{dissolve}}{\partial \mu^s} \right)_{E_{ij}, \bar{p}, \mu}$$

$$X = \left(\frac{\partial m_{bound}}{\partial \mu^s} \right)_{E_{ij}, \bar{p}, \mu} = -\left(\frac{\partial m_{dissolve}}{\partial \mu} \right)_{E_{ij}, \bar{p}, \mu^s}$$

$$B^s = - \left(\frac{\partial m_{dissolve}}{\partial \bar{p}} \right)_{E_{ij}, m, m^s} = \left(\frac{\partial m_{bound}}{\partial m^s} \right)_{E_{ij}, \bar{p}, m}$$

Equations (28)-(31) provide the general coupled equations for mechanical behaviour, water pressure, and chemical potential, etc. As the attention of this article is focused on the coupled dissolution and swelling influence for unsaturated swelling rock, a few assumptions are made including

i) Small strains assumption. This leads to the replacement of Green Strain tensor E_{ij} by strain tensor ε_{ij}, and Piola-Kirchhoff stress T_{ij} by Cauchy stress σ_{ij}.

ii) Materials parameters assumption. The parameters L_{ijkl}, M_{ij}, S_{ij}, Z, B, Q, X, Y are material-dependent constants and the material is isotropic. Hence, the tensors M_{ij}, S_{ij}, H_{ij} are diagonal and can be written in the forms of scalars ζ, ω, w_s as

$$M_{ij} = \zeta \delta_{ij}, S_{ij} = \omega \, \delta_{ij}, H_{ij} = w_s d_{ij} \tag{33}$$

iii) Based on the assumption ii), the elastic stiffness L_{ijkl} can be a fourth-order isotropic tensor

$$L_{ijkl} = G(\delta_{ik}\delta_{jl} + \delta_{il}\delta_{jk}) + (K - \frac{2G}{3})\delta_{ij}\delta_{kl} \quad (34)$$

Here G denotes the rock's shear modulus and K denotes the bulk modulus.

4 Coupled hydro-mechanical constitutive equations

4.1 Mechanical behaviour

Based on the material parameters simplification from i-iii in section 3.3, the governing stress equation (28) can be simplified to

$$\dot{\sigma}_{ij} = (K - \frac{2G}{3})\dot{\varepsilon}_{kk}\delta_{ij} + 2G\dot{\varepsilon}_{ij} - z\dot{\bar{p}}\delta_{ij} + w_d\dot{d}_{kl} - w_s n\dot{\delta}_{kl} \tag{35}$$

where K_s is the bulk modulus of the solid matrix.The quantity z is related to the bulk modulus K and K_s in a manner from poroelasticity through the equation $\zeta = 1-(K/K_s)$ namely.

By introducing equation(17) into equation (35), and assuming the linear relationship $\dot{\mu}^s = x\,\dot{\mu}$, then the stress equation (35) can be rewritten as

$$\dot{\sigma}_{ij} = (K - \frac{2G}{3})\dot{\varepsilon}_{kk}\delta_{ij} + 2G\dot{\varepsilon}_{ij} - (z - \frac{w}{(x+1)S^w r_t^w} + \frac{(x+1)w_d}{xS^w r_t^w})\dot{\bar{p}}\delta_{ij} \tag{36}$$

Under mechanical equilibrium condition $\partial\sigma_{ij}/\partial x_j = 0$, and using displacement variables $d_i (i = 1,2,3)$ through $\varepsilon_{ij} = \frac{1}{2}(d_{i,j} + d_{j,i})$, equation (36) can be written as

$$G\tilde{N}^2\mathbf{d} + \left(\frac{G}{1-2q}\right)\tilde{N}(\tilde{N}\cdot\mathbf{d}) - (z - \frac{w}{(x+1)S^w r_t^w} + \frac{(x+1)w_d}{xS^w r_t^w})\tilde{N}\dot{\bar{p}} = 0 \tag{37}$$

Since the average pressure $\bar{p}$ can be interpreted as $\bar{p} = S^w p^w$ (Li and Zienkiewicz, 1992) and its time derivative is

$$\dot{\bar{p}} = S^w\frac{\partial p^w}{\partial t} + \frac{C_s}{f}p^w\frac{\partial p^w}{\partial t} = (S^w + \frac{C_s}{f}p^w)\frac{\partial p^w}{\partial t} \tag{38}$$

where $\bar{C}_s$ in the specific moisture content that is defined in terms of pressure.

By introducing equation (38), equation (37) can be rewritten as

$$G\nabla^2\mathbf{d} + \frac{G}{1-2\nu}\nabla(\nabla\cdot\mathbf{d}) - (z - \frac{w}{(x+1)S^w\rho_t^w} + \frac{(x+1)w_d}{xS^w\rho_t^w})\nabla\left[(S^w + \frac{C_s}{f}p^w)p^w\right] = 0 \tag{39}$$

Equation (39) presents a formula including both the swelling and dissolution influence on mechanical behaviour.

4.2 Fluid-phase

From the water balance equation (8), water density equation (9) and Euler identity, the conservation equation of water is

$$(S^w\dot{\rho}_t^w) + \nabla\cdot(\rho_t^w\dot{\mathbf{u}}) = 0 \tag{40}$$

From equation (40), (4) and (13), it leads to

$$\begin{aligned} &S^w\rho_t^w z\nabla\cdot\dot{\mathbf{d}} + S^w\rho_t^w(Q + B/\rho_t^w)\dot{p}^w \\ &+ f\rho_t^w\frac{\partial S^w}{\partial t} + fS^w\frac{\partial\rho_t^w}{\partial t} + \rho_t^w\left[k\frac{k_{rw}}{\nu}\nabla^2 p_w\right] = 0 \end{aligned} \tag{41}$$

Where Q is the void compressibility, relating to the scalar z through $Q = (1/K_s)/(\zeta - \phi)$, in which K_s is the bulk modulus of the solid matrix which is here assumed to be very large, and $B = (1/K)(z-1)w$.

Considering the rate of change of saturation function and the rate of change of water density function

$$\phi\frac{\partial S^w}{\partial t} + \frac{\phi S^w}{\rho_t^w}\frac{\partial\rho_t^w}{\partial t} = C_S\frac{\partial p^w}{\partial t} + \phi\frac{S^w}{K_w}\frac{\partial p^w}{\partial t} = (C_S + \phi\frac{S^w}{K_w})\frac{\partial p^w}{\partial t} \tag{42}$$

equation (41) can be rewritten as

$$-k\frac{k_{rw}}{\nu}\nabla^2 p_w + (C_S + f\frac{S^w}{K_w})\frac{\partial p^w}{\partial t} + S^w(Q + B/\rho_t^w)(S^w + \frac{C_s}{f}p^w)\frac{\partial p^w}{\partial t} + S^w z\nabla\cdot\dot{\mathbf{d}} = 0 \tag{43}$$

4.3 Equation summary and validation

The coupled equations (39) and (43) can be validated by the comparing with unsaturated hydro-mechanical coupled equations derived from the mechanics approach which have been tested by number of researchers. Without considering swelling and dissolution, equations (39) and (43) become the classic equations from mechanics approach (Lewis and Schrefler, 1987a). The difference is coupled swelling and dissolution term $-\frac{w}{(x+1)S^{w}r_{t}^{w}}+\frac{(x+1)w_{d}}{xS^{w}r_{t}^{w}}$, and these two terms can be determined by experiment.

5 Numerical simulation

In this section, numerical modelling is presented to show the coupled hydro-mechanical behaviour with consideration of swelling and dissolution for a host rock around a nuclear waste container. The host rock for a nuclear waste works as a barrier to prevent radionuclides from leaching into the biosphere via underground water.

5.1 Conceptual model

5.1.1 Model geometry and material parameters. Figure 3 shows a simplified one-dimensional model geometry (0.015m wide and 0.03m high) representing a host rock (not in scale). Boundary A is fixed and permeable, and boundary B is free and permeable. The upper and lower boundaries are on rollers allowing only horizontal displacement.

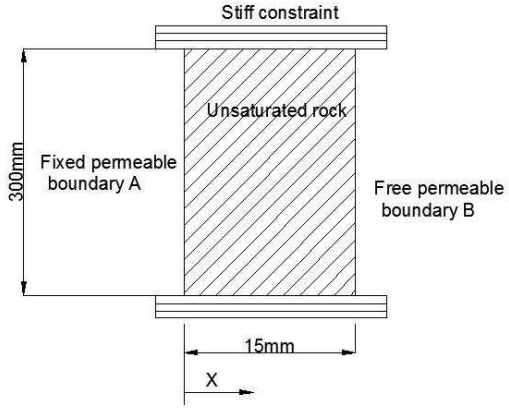

Fig 3. Numerical modelling geometry and boundary condition

5.1.2 Initial and boundary condition. The domain is assumed to contain water at a pressure of -4MPa (unsaturated condition), with the corresponding degree of saturation as 0.995 obtained through using Van Genuchten relationship as

$$k_{rw} = \left(S^{w}\right)^{0.5}\left[1-\left(1-\left(S^{w}\right)^{1/m}\right)^{m}\right]^{2}$$

$$S^{w} = \left[\left(-P/M\right)^{1/(1-m)}+1\right]^{-m}$$

The whole domain is in equilibrium and the effective stress is zero.

5.1.3 Dissolution/Swelling, and parameters

In equation(39), a dissolution term dv= $\frac{(x+1)w_d}{xS^w r_t^w}$, and a swelling term

sw= $\frac{w}{(x+1)S^w r_t^w}$ have been included to account for the dissolution and swelling process. In realistic conditions, both dissolution and swelling are time-dependent processes. To simplify the analysis, the dissolution and swelling term are assumed to be constant as dv=0.05 and sw=0.2, respectively. The material parameters are listed in table 1.

Table 1 material parameters (Chen, 2013)

Parameters	Physical meaning	Values and units
r_t^w	Density of water	1000kg/m^3
k/v	absolute permeability/dynamic viscosity	10^{-14}m/s
m	Van Genuchten parameter	0.43
M	Van Genuchten parameter	51Mpa
E	Young's modulus	9720MPa
θ	Poisson's ratio	0.2
z	Biot's coefficient	1
Q	Void compressibility	0.000005MPa^{-1}
S_w	Swelling parameter	0.2
dv	Dissolution parameter	0.05

5.2 Numerical result

At the beginning of the simulation, the pore water pressure at boundary A drops from -4MPa to -20MPa. Pore water pressure and degree of saturation are maintained to be

the initial value at boundary B. The software COMSOL is used to solve the coupled constitutive equation.

5.2.1 pore water pressure and degree of saturation

Fig 4 and Fig 5 shows the distribution of pore water pressure and saturation throughout the domain at different time. Because there is a direct link between pore water pressure and saturation through Van Genuchten relationship, the two figures show a similar trend. As the absolute permeability is assumed to be constant, and swelling/dissolution are assumed to have little influence on the absolute and relative permeability, the pore pressure remains the same for both swelling (sw=0.2) and non-swelling (sw=0), dissolving (dv=0.05) and non-dissolving(dv=0) rocks.

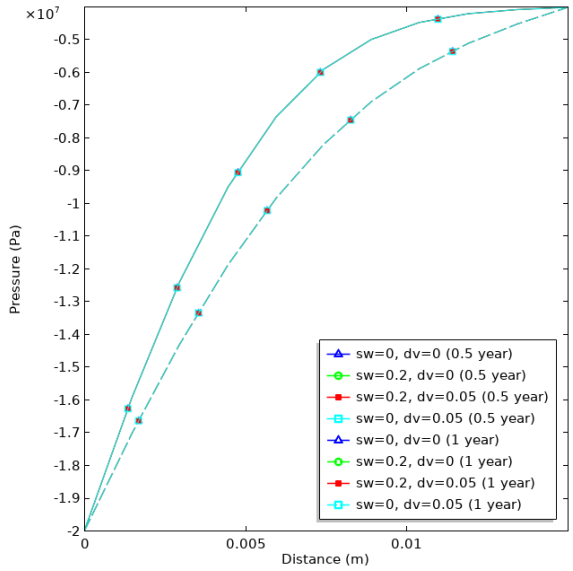

Fig 4. Evolution of pore water pressure with time

(solid line: t=0.5 year, dashed line: t=1 year)

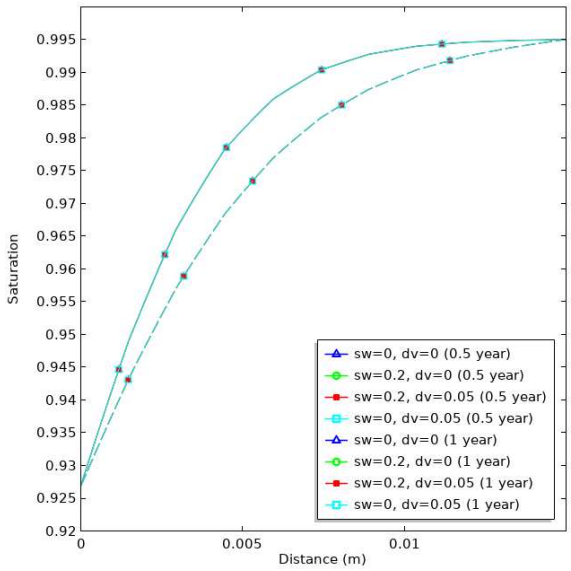

Fig 5. Evolution of saturation distribution with time

(solid line: t=0.5 year, dashed line: t=1 year)

5.2.2 Effective stress, strain, and displacement

Fig 6 shows the change of horizontal effective stress. Effective stress at boundary B remains 0. At boundary A, “swelling and non-dissolving rock” has the smallest effective stress, while “non-swelling and dissolving rock” has the largest effective stress. Compare different lines in Fig 6, it can be concluded that swelling process decreases effective stress and the dissolving process increases effective stress. This is because swelling effect reduces the total stress influence on the solid skeleton whereas dissolution effect enlarges such influence. A similar trend can be found in horizontal strain and displacement (Figs 7 and 8). Since swelling and dissolution process have contrary effects on the rock, the deformation of the rock depends on the combined impact of swelling and dissolution (Figs 8)

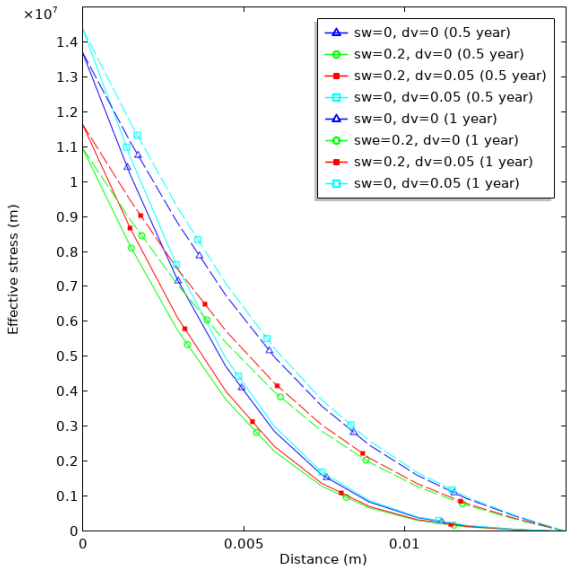

Fig 6. Evolution of effective stress with time

(solid line: t=0.5 year, dashed line: t=1 year)

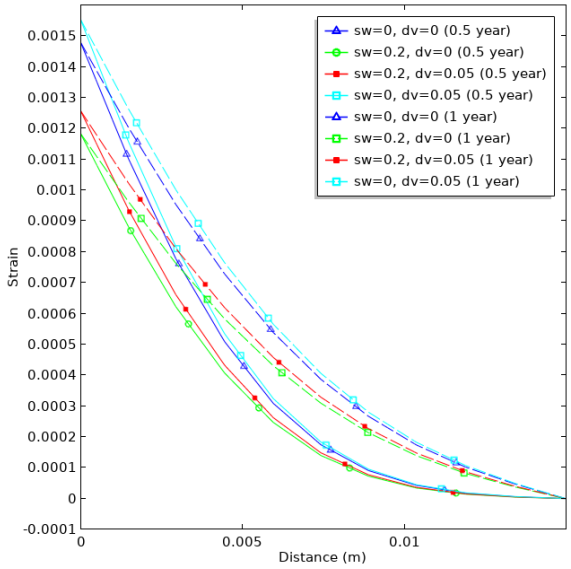

Fig 7. Evolution of horizontal strain with time

(solid line: t=0.5 year, dashed line: t=1 year)

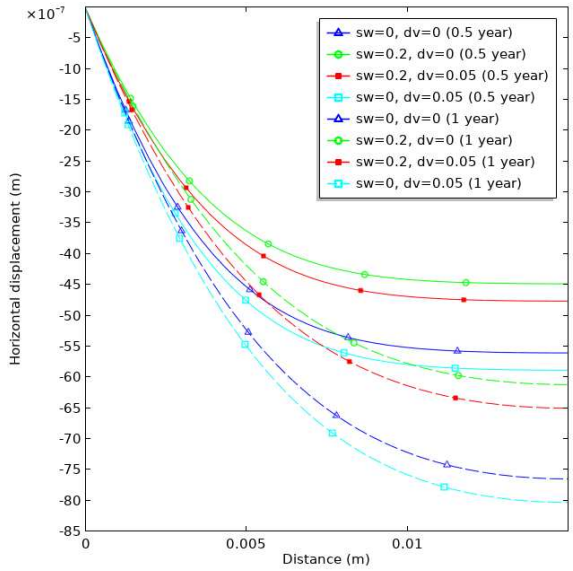

Fig.8 Evolution of horizontal displacement with time (sw=0.2, dv=0.05)

(solid line: t=0.5 year, dashed line: t=1 year)

5.3 Sensitivity analysis of permeability parameter

Permeability is very important in H-M coupling. This section compares the influence of "swelling + dissolving" on the deformation of rocks, under different permeability: $\mathrm{k}/\theta = 10^{-13}$ and $\mathrm{k}/\theta = 10^{-14}$ at 0.5 years (Note, k is used in the figures' label to represent k/θ). The pore water pressure and saturation change much faster at large permeability ($\mathrm{k}/\theta = 10^{-13}$) (Figs 9 and 10). Effective stress, horizontal strain, and displacement in high permeability ($\mathrm{k}/\theta = 10^{-13}$) rock are all larger in low permeability ($\mathrm{k}/\theta = 10^{-14}$) (Figs 11-13) at the same time (0.5 years) due to the faster increase of water pressure caused by higher permeability.

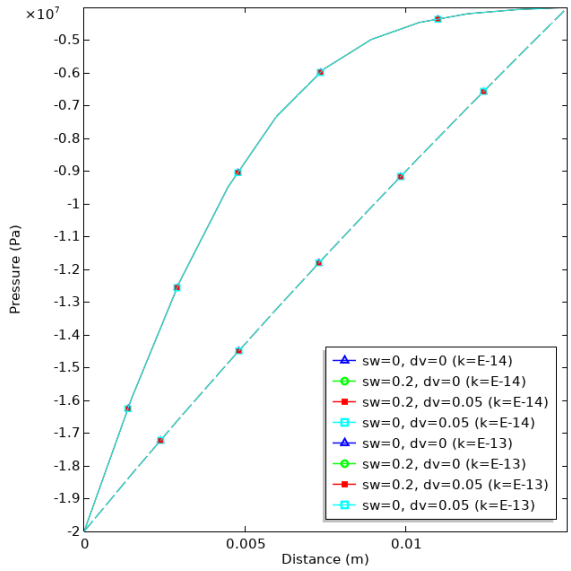

Fig 9. Evolution of pore water pressure with time

(solid line: $k/\theta = 10^{-14}$, dashed line: $k/\theta = 10^{-13}$)

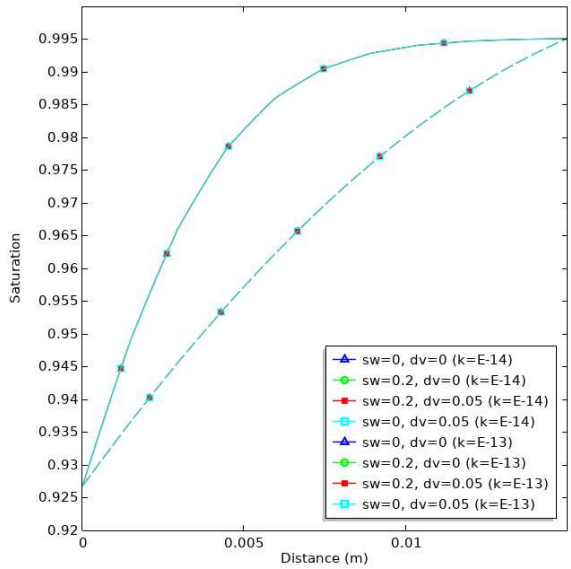

Fig 10. Evolution of saturation with time

(solid line: $k/\theta = 10^{-14}$, dashed line: $k/\theta = 10^{-13}$)

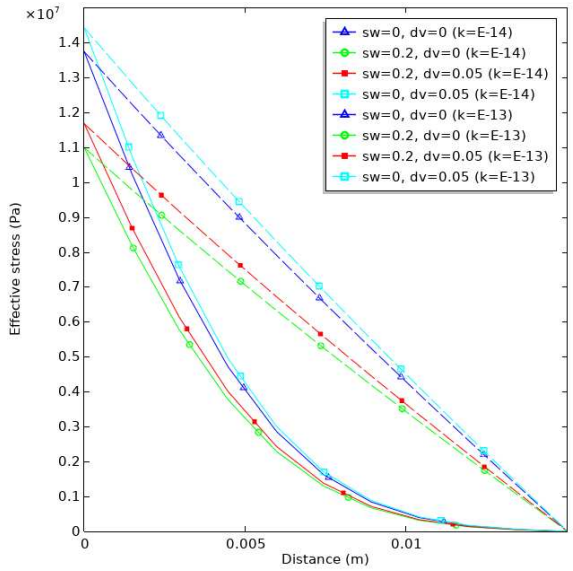

Fig 11. Evolution of effective stress with time

(solid line: $k/\theta = 10^{-14}$, dashed line: $k/\theta = 10^{-13}$)

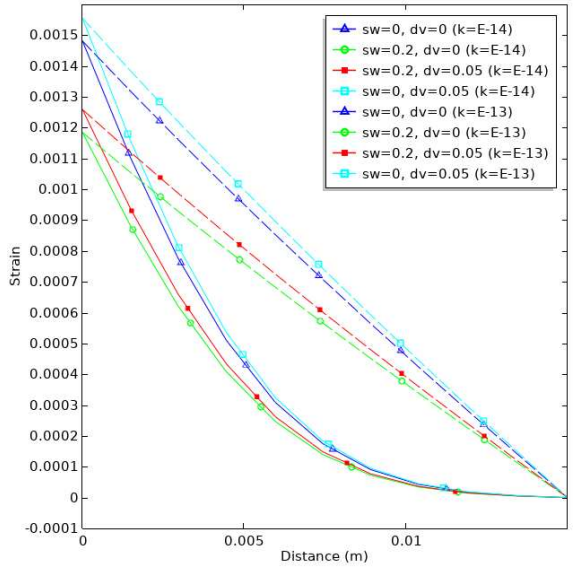

Fig 12. Evolution of horizontal strain with time

(solid line: $k/\theta = 10^{-14}$, dashed line: $k/\theta = 10^{-13}$)

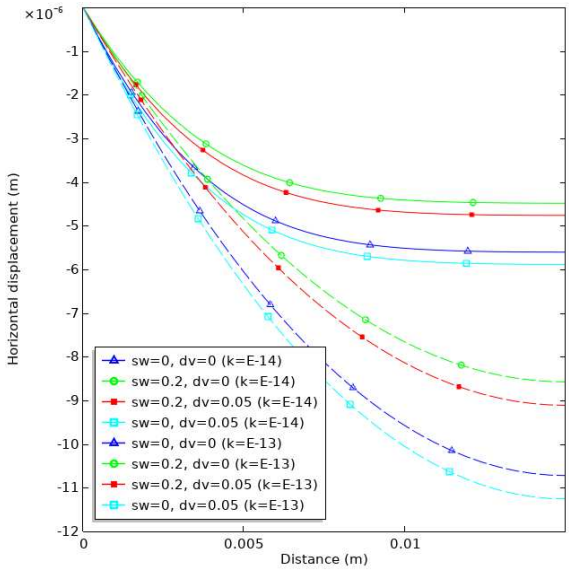

Fig 13. Evolution of horizontal displacement with time

(solid line: $k/\theta = 10^{-14}$, dashed line: $k/\theta = 10^{-13}$)

5.4 2D numerical simulation

The above 1D model has demonstrated the influence of swelling and dissolution. A 2D model is presented for a comprehensive analysis. The parameters and initial conditions are the same as those used in the 1D model, the major difference is that the pressure boundary conditions (Figure 14): The water pressure at boundary A decreases from -4E6 to -20E6 (Pa) representing an excavation process, whereas, the pressure at boundary B changes from the initial constant value of -4E6 to a linear distribution along the hight of the sample (-4E6 to -10E6) representing an underground water flow changing scenario.

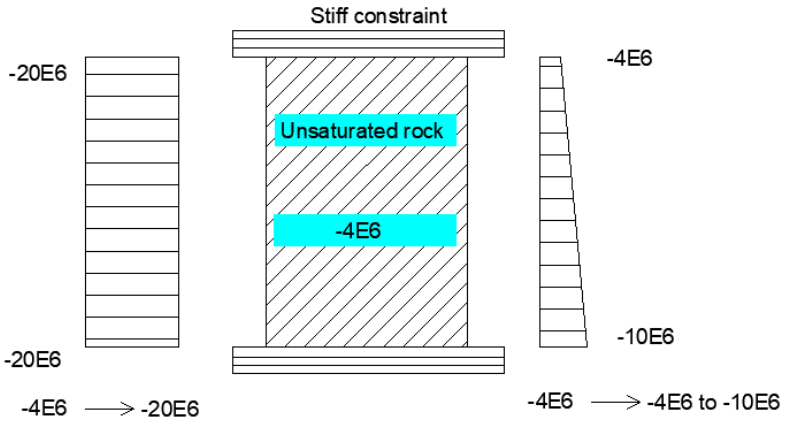

Fig 14. Boundary conditions for the 2-D model

Fig 15 shows the pressure distribution at different times for a rock with combined swelling and dissolving function. Water in the domain flows out via the boundary A (left) and water pressure decreases to -20E6 . Because the linear function of pressure on boundary B (right), it leads to a pressure change along with the height within the domain.

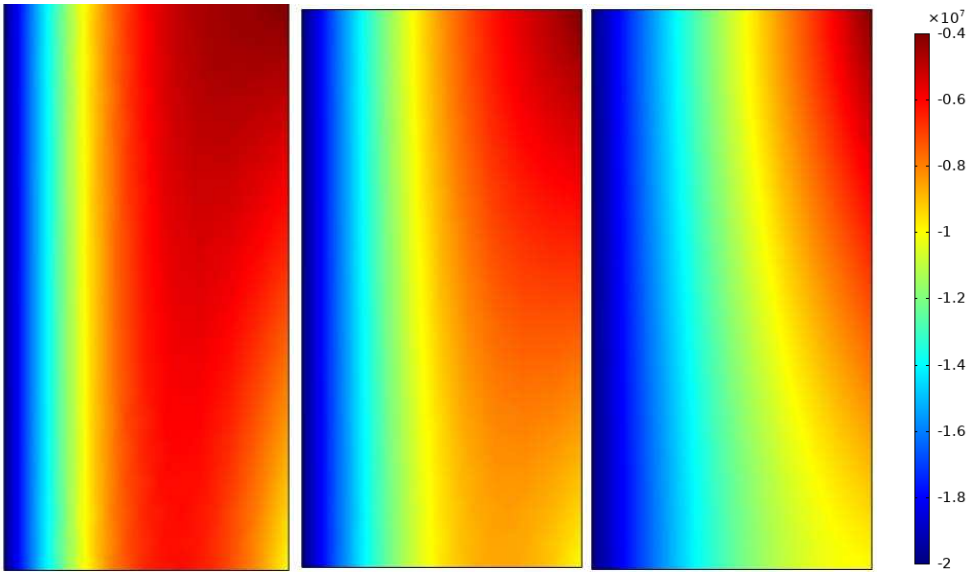

(a) (b) (c)

Fig 15. Pressure distribution at different time(sw=0.2, dv=0.05)

((a). t=0.5 year, (b). t=1 year, (c). t=2 years)

Fig 16 shows the displacement changes at different times. The displacement at the boundary A remains 0 as it is fixed. The displacement at the top right (boundary B) is the largest as the pressure gradient is the largest. A displacement variation against the height can be observed.

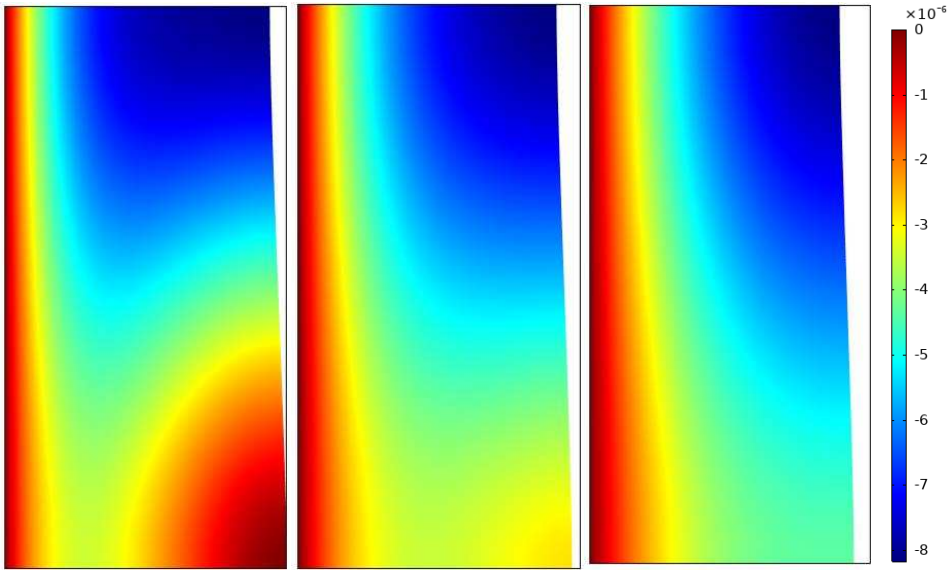

(a) (b) (c)

Fig 17. Horizontal displacement distribution at different time(sw=0.2, dv=0.05)

((a). t=0.5 year, (b). t=1 year, (c). t=2 years)

5.5 Limitation of the numerical analysis and further work

The numerical simulation presented here is a simplified case for the demonstration purpose of the complex mathematical equations, with the assumptions made as 1) Swelling and dissolution do not impact permeability (or porosity) nor concentrations, which presents only in very high saturation ratio and low kinetics reaction in short period of time (e.g. < 1 year for quartz dissolution); 2) Variations of chemical potential of water and of dissolved solid are linearly related. This only presents in the condition of low concentration of dissolved solids. The relationship between chemical potential of water and of dissolved solid can be further modified according to a real situation; 3)

The dissolution and swelling terms are assumed to be constant, however, they are functions of the state variables and need to be determined by experiments.

This paper focuses on the derivation of the governing equations, presenting a simple numerical simulation only for demonstration purposes. A more realistic and complex numerical simulation for nuclear waste disposal applications will be presented in another paper.

6 Conclusions

This paper extends the Biot's elasticity theory by including the molecular influence from swelling and dissolution based on mixture coupling theory. A general coupled structure for swelling and dissolvable materials has been formed. The rigorous derivation obtained by using mixture coupling theory gives a deep insight of the inter-effects between molecular reaction, rock deformation, pore water, and water molecules in the clay platelets.

The numerical simulation analyzes the influence of swelling and dissolution processes on the deformation of an unsaturated rock sample. The numerical results show that swelling and dissolution have a contrary influence on the rock deformation. The research has been focussed on unsaturated water flow without considering chemicals transport, which is important for the nuclear waste disposal industry and will be conducted in future research.

Acknowledgment

The authors would like to acknowledge the contribution of Professor Doug Stewart on this paper, and would like to acknowledge the financial support of CERES international studentship from the School of Civil Engineering at the University of Leeds.

Appendix

This appendix gives a detailed deviation process for equations (28)-(31).

$$\dot{T}_{ij} = \frac{\partial T_{ij}}{\partial t} = \frac{\partial}{\partial t}\left(\frac{\partial W}{\partial E_{ij}}\right)_{\bar{p},\mu,\mu^s} = \left(\frac{\partial}{\partial E_{ij}}\left(\frac{\partial W}{\partial t}\right)\right)_{\bar{p},\mu,\mu^s} = \left(\frac{\partial \dot{W}}{\partial E_{ij}}\right)_{\bar{p},\mu,\mu^s} \tag{44}$$

Substituting equation (27) into equation (44) leads to

$$\begin{aligned}
\dot{T}_{ij} &= \left(\frac{\partial}{\partial E_{ij}}\left(\left(\frac{\partial W}{\partial E_{ij}}\right)_{\bar{p},\mu,\mu^s}\dot{E}_{ij} + \left(\frac{\partial W}{\partial \bar{p}}\right)_{E_{ij},\mu,\mu^s}\dot{\bar{p}} + \left(\frac{\partial W}{\partial \mu}\right)_{E_{ij},\bar{p},\mu^s}\dot{\mu} + \left(\frac{\partial W}{\partial \mu^s}\right)_{E_{ij},\bar{p},\mu}\dot{\mu}^s\right)\right)_{\bar{p},\mu,\mu^s} \\
&= \left(\frac{\partial}{\partial E_{ij}}\left(\frac{\partial W}{\partial E_{ij}}\right)_{\bar{p},\mu,\mu^s}\right)_{\bar{p},\mu,\mu^s}\dot{E}_{ij} + \left(\frac{\partial}{\partial E_{ij}}\left(\frac{\partial W}{\partial \bar{p}}\right)_{E_{ij},\mu,\mu^s}\right)_{\bar{p},\mu,\mu^s}\dot{\bar{p}} \\
&+ \left(\frac{\partial}{\partial E_{ij}}\left(\frac{\partial W}{\partial \mu}\right)_{E_{ij},\bar{p},\mu^s}\right)_{\bar{p},\mu,\mu^s}\dot{\mu} + \left(\frac{\partial}{\partial E_{ij}}\left(\frac{\partial W}{\partial \mu^s}\right)_{E_{ij},\bar{p},\mu}\right)_{\bar{p},\mu,\mu^s}\dot{\mu}^s \\
&= \left(\frac{\partial^2 W}{\partial E_{ij}\partial E_{kl}}\right)_{\bar{p},\mu,\mu^s}\dot{E}_{ij} + \left(\frac{\partial^2 W}{\partial \bar{p}\partial E_{ij}}\right)_{\mu,\mu^s}\dot{\bar{p}} + \left(\frac{\partial^2 W}{\partial \mu\partial E_{ij}}\right)_{\bar{p},\mu^s}\dot{\mu} + \left(\frac{\partial^2 W}{\partial \mu^s\partial E_{ij}}\right)_{\bar{p},\mu}\dot{\mu}^s \\
&= \left(\frac{\partial T_{ij}}{\partial E_{kl}}\right)_{\bar{p},\mu,\mu^s}\dot{E}_{ij} - \left(\frac{\partial \upsilon}{\partial E_{ij}}\right)_{\bar{p},\mu,\mu^s}\dot{\bar{p}} - \left(\frac{\partial m_{bound}}{\partial E_{ij}}\right)_{\bar{p},\mu,\mu^s}\dot{\mu} + \left(\frac{\partial m_{dissolve}}{\partial E_{ij}}\right)_{\bar{p},\mu,\mu^s}\dot{\mu}^s
\end{aligned} \tag{45}$$

Following the similar logic as the derivation of $\dot{T}_{ij}$, the equations for $\dot{u}$, $\dot{m}_{bound}$ and $\dot{m}_{dissolve}$ can be obtained as

$$\begin{aligned}
\dot{u} &= -\left(\frac{\partial}{\partial \bar{p}}\left(\frac{\partial W}{\partial E_{ij}}\right)_{\bar{p},m,m^s}\right)\dot{E}_{ij} + \left(\frac{\partial W}{\partial \bar{p}}\right)_{E_{ij},m,m^s}\dot{\bar{p}} + \left(\frac{\partial W}{\partial m}\right)_{E_{ij},\bar{p},m^s}\dot{m} + \left(\frac{\partial W}{\partial m^s}\right)_{E_{ij},\bar{p},m}\dot{m}^s \\
&= -\left(\frac{\partial^2 W}{\partial E_{ij}\partial \bar{p}}\right)_{m,m^s}\dot{E}_{ij} - \left(\frac{\partial^2 W}{\partial \bar{p}\partial \bar{p}}\right)_{E_{ij},m,m^s}\dot{\bar{p}} + \left(\frac{\partial^2 W}{\partial m\partial \bar{p}}\right)_{E_{ij},m^s}\dot{m} + \left(\frac{\partial^2 W}{\partial m^s\partial \bar{p}}\right)_{E_{ij},m}\dot{m}^s \\
&= -\left(\frac{\partial T_{ij}}{\partial \bar{p}}\right)_{E_{ij},m,m^s}\dot{E}_{ij} + \left(\frac{\partial u}{\partial \bar{p}}\right)_{E_{ij},m,m^s}\dot{\bar{p}} + \left(\frac{\partial m_{bound}}{\partial \bar{p}}\right)_{E_{ij},m,m^s}\dot{m} + \left(\frac{\partial m_{dissolve}}{\partial \bar{p}}\right)_{E_{ij},m,m^s}\dot{m}^s
\end{aligned} \tag{46}$$

$$\begin{aligned}
\dot{m}_{bound} &= -\left(\frac{\partial}{\partial \bar{p}}\left(\frac{\partial W}{\partial E_{ij}}\right)_{\bar{p},m^s}\right)\dot{E}_{ij} - \left(\frac{\partial W}{\partial \bar{p}\partial m}\right)_{E_{ij},m^s}\dot{\bar{p}} + \left(\frac{\partial W}{\partial m\partial m}\right)_{E_{ij},\bar{p},m^s}\dot{m} + \left(\frac{\partial W}{\partial m^s\partial m}\right)_{E_{ij},\bar{p}}\dot{m}^s \\
&= -\left(\frac{\partial T_{ij}}{\partial m}\right)_{E_{ij},\bar{p},m^s}\dot{E}_{ij} + \left(\frac{\partial u}{\partial m}\right)_{E_{ij},\bar{p},m^s}\dot{\bar{p}} + \left(\frac{\partial m_{bound}}{\partial m}\right)_{E_{ij},\bar{p},m^s}\dot{m} + \left(\frac{\partial m_{dissolve}}{\partial m}\right)_{E_{ij},\bar{p},m^s}\dot{m}^s
\end{aligned} \tag{47}$$

$$\dot{m}_{dissolve} = \left(\frac{\partial^2 W}{\partial E_{ij} \partial m^s}\right)_{\bar{p},m} \dot{E}_{ij} + \left(\frac{\partial^2 W}{\partial \bar{p} \partial m^s}\right)_{E_{ij},m} \dot{\bar{p}} + \left(\frac{\partial^2 W}{\partial m \partial m^s}\right)_{E_{ij},\bar{p}} \dot{m} + \left(\frac{\partial^2 W}{\partial m^s \partial m^s}\right)_{E_{ij},\bar{p},m} \dot{m}^s$$
$$= \left(\frac{\partial T_{ij}}{\partial m^s}\right)_{E_{ij},\bar{p},m} \dot{E}_{ij} - \left(\frac{\partial u}{\partial m^s}\right)_{E_{ij},\bar{p},m} \dot{\bar{p}} + \left(\frac{\partial m_{bound}}{\partial m^s}\right)_{E_{ij},\bar{p},m} \dot{m} + \left(\frac{\partial m_{dissolve}}{\partial m^s}\right)_{E_{ij},\bar{p},m} \dot{m}^s \quad (48)$$

REFERENCES

Biot, M.A., 1962. Mechanics of deformation and acoustic propagation in porous media. Journal of applied physics 33, 1482-1498.

Biot, M.A., Temple, G., 1972. Theory of finite deformations of porous solids. Indiana University Mathematics Journal 21, 597-620.

Chen, X., 2010. Unsaturated hydro-chemo-mechanical modelling based on modified mixture theory.

Chen, X., 2013. Constitutive unsaturated hydro-mechanical model based on modified mixture theory with consideration of hydration swelling. International Journal of Solids and Structures 50, 3266-3273.

Chen, X., Hicks, M.A., 2009. Influence of water chemical potential on the swelling of water sensitive materals. Computers and Structures In press.

Chen, X., Hicks, M.A., 2010. Influence of water chemical potential on the swelling of water sensitive materials. Computers & structures 88, 1498-1505.

Chen, X., Pao, W., Thornton, S., Small, J., 2016. Unsaturated hydro-mechanical–chemical constitutive coupled model based on mixture coupling theory: Hydration swelling and chemical osmosis. International Journal of Engineering Science 104, 97-109.

Chen, X., Thornton, S.F., Pao, W., 2018a. Mathematical model of coupled dual chemical osmosis based on mixture-coupling theory. International Journal of Engineering Science 129, 145-155.

Chen, X., Thornton, S.F., Small, J., 2015. Influence of Hyper-Alkaline pH Leachate on Mineral and Porosity Evolution in the Chemically Disturbed Zone Developed in the Near-Field Host Rock for a Nuclear Waste Repository. Transport in Porous Media 107, 489-505.

Chen, X., Wang, M., Hicks, M.A., Thomas, H.R., 2018b. A new matrix for multiphase couplings in a membrane porous medium. International Journal for Numerical and Analytical Methods in Geomechanics.

Emmanuel, S., Berkowitz, B., 2007. Effects of pore-size controlled solubility on reactive transport in heterogeneous rock. Geophysical Research Letters 34.

Fredd, C.N., Fogler, H.S., 1998. Influence of transport and reaction on wormhole formation in porous media. AIChE journal 44, 1933-1949.

Grasley, Z., Rajagopal, K., Leung, C., 2011. Equilibrium of partially dried porous media influenced by dissolved species and the development of new interfaces. International Journal of Engineering Science 49, 711-725.

Grasley, Z.C., Rajagopal, K.R., 2012. Revisiting total, matric, and osmotic suction in partially saturated geomaterials. Zeitschrift für angewandte Mathematik und Physik 63, 373-394.

Gray, W.G., Miller, C.T., 2014. Introduction to the thermodynamically constrained averaging theory for porous medium systems. Springer.

Gray, W.G., Miller, C.T., Schrefler, B.A.J.A.i.w.r., 2013. Averaging theory for description of environmental problems: What have we learned? 51, 123-138.

Graziani, A., Boldini, D., 2011. Influence of hydro-mechanical coupling on tunnel response in clays. Journal of Geotechnical and Geoenvironmental Engineering 138, 415-418.

Haase, R., 1990. Thermodynamics of irreversible processes. Dover, New York.

Heidug, W., Wong, S.W., 1996. Hydration swelling of water-absorbing rocks: a constitutive model. International Journal for Numerical and Analytical Methods in Geomechanics 20, 403-430.

Humphrey, J., Rajagopal, K., 2002. A constrained mixture model for growth and remodeling of soft tissues. Mathematical models and methods in applied sciences 12, 407-430.

Humphrey, J., Rajagopal, K., 2003. A constrained mixture model for arterial adaptations to a sustained step change in blood flow. Biomechanics and modeling in mechanobiology 2, 109-126.
Huyghe, J., Janssen, J., 1999. Thermo-chemo-electro-mechanical formulation of saturated charged porous solids. Transport in Porous Media 34, 129-141.
Israelachvili, J.N., 1991. Intermolecular and surface forces. Academic Press, London.
Katachalsky, A., Curran, P.F., 1965. Nonequilibrium thermodynamics in biophysics. Harvard University Press, Cambridge, MA.
Laloui, L., Klubertanz, G., Vulliet, L., 2003. Solid–liquid–air coupling in multiphase porous media. International Journal for Numerical and Analytical Methods in Geomechanics 27, 183-206.
Lewis, R.W., Schrefler, B.A., 1987a. The finite-element method in deformation and consolidation of porous media. Wiley, New York.
Lewis, R.W., Schrefler, B.A., 1987b. The finite element method in the deformation and consolidation of porous media.
Li, X., Zienkiewicz, O.C., 1992. Multiphase flow in deforming porous media and finite element solutions. Comput. Struct. 45, 2l 1-227.
Meroi, E., Schrefler, B., Zienkiewicz, O., 1995. Large strain static and dynamic semisaturated soil behaviour. International Journal for Numerical and Analytical Methods in Geomechanics 19, 81-106.
Miller, C., Gray, W., Kees, C.J.E., 2018. Thermodynamically constrained averaging theory: principles, model hierarchies, and deviation kinetic energy extensions. 20, 253.
Moyce, E.B., Rochelle, C., Morris, K., Milodowski, A.E., Chen, X., Thornton, S., Small, J.S., Shaw, S.J.A.G., 2014. Rock alteration in alkaline cement waters over 15 years and its relevance to the geological disposal of nuclear waste. 50, 91-105.
Neuman, S.P., 1975. Galerkin approach to saturated–unsaturated flow in porous media, in: Gallagher, R.H., Oden, J.T., Taylor, C., Zienkiewicz, O.C. (Eds.), Finite Elements in Fluids. John Wiley & Sons, New York.
NNL, 2016. Summary of the BIGRAD project and its implications for a geological disposal facility, A report prepared for and on behalf of Radioactive Waste Management Ltd.
Rajagopal, K., 2007. On a hierarchy of approximate models for flows of incompressible fluids through porous solids. Mathematical Models and Methods in Applied Sciences 17, 215-252.
Rajagopal, K., Tao, L., 2005. On the propagation of waves through porous solids. International Journal of Non-Linear Mechanics 40, 373-380.
Rajagopal, K.R., Tao, L., 1995. Mechanics of mixtures. World scientific.
Safai, N.M., Pinder, G.F., 1979. Vertical and horizontal land deformation in a desaturating porous medium. Adv. Water Res. 2, 19-25.
Sanavia, L., Schrefler, B., Steinmann, P., 2002. A formulation for an unsaturated porous medium undergoing large inelastic strains. Computational Mechanics 28, 137-151.
Seetharam, S., Thomas, H., Cleall, P.J., 2007. Coupled thermo/hydro/chemical/mechanical model for unsaturated soils—Numerical algorithm. International Journal for Numerical Methods in Engineering 70, 1480-1511.
Terzaghi, K., 1943. Theory of consolidation. Theoretical Soil Mechanics, 265-296.
Yadav, S.K., Chakrapani, G., 2006. Dissolution kinetics of rock–water interactions and its implications. Current Science, 932-937.
Zhao, C., 2014. Physical and chemical dissolution front instability in porous media. Cham, Switzerland: Springer.